Journal of Photochemistry & Photobiology, B: Biology 226 (2022) 112368

Contents lists available at ScienceDirect

Journal of Photochemistry & Photobiology, B: Biology

journal homepage: www.elsevier.com/locate/jphotobiol

Nitrogen-limitation exacerbates the impact of ultraviolet radiation on the coccolithophore *Gephyrocapsa oceanica*

Xiaowen Jiang [a], Yong Zhang [a,c], David A. Hutchins [d], Kunshan Gao [a,b,*]

[a] State Key Laboratory of Marine Environmental Science & College of Ocean and Earth Sciences, Xiamen University, Xiamen, China
[b] Co-Innovation Center of Jiangsu Marine Bio-industry Technology, Jiangsu Ocean University, Lianyungang 222005, China
[c] College of Environmental Science and Engineering and Fujian Key Laboratory of Pollution Control and Resource Recycling, Fujian Normal University, Fuzhou, China
[d] Marine and Environmental Biology, University of Southern California, Los Angeles, CA, United States

ARTICLE INFO

Keywords:
Calcification
Coccolithophore
Growth
Gephyrocapsa oceanica
Nitrate-limitation
Photosynthesis
Phytoplankton
UVR

Abstract: To investigate effects of UV radiation (UVR, 280–400 nm) on coccolithophorids under nutrient-limited conditions, we grew *Gephyrocapsa oceanica* to determine its resilience to consecutive daily short-term exposures to +UVR (irradiances >295 nm) under a range of nitrate availabilities (100, 24, 12, 6 and 3 μM). +UVR alone significantly hampered the growth of *G. oceanica*, with the synergistic negative effects of +UVR and N-limitation being about 58% and 22% greater than under UVR or N-limitation alone, respectively. Most 3 μM nitrate cultures died, but those exposed to UVR succumbed sooner. This was due to a failure of photoprotection and repair mechanisms under low N-availability with exposures to UVR. Additionally, the UVR-induced inhibition of the effective quantum yield of photosystem II (PSII) was significantly higher and was further aggravated by N limitation. The algal cells increased photoprotective pigments and UV-absorbing compounds as a priority rather than using calcification for defense against UVR, indicating a trade-off in energy and resource allocation. Our results indicate the negative effects of UVR on coccolithophorid growth and photosynthesis, and highlight the important role of N availability in defense against UVR as well as high PAR. We predict that enhanced N-limitation in future surface oceans due to warming-induced stratification will exacerbate the sensitivity of *G. oceanica* to UVR, while coccolithophores can be potentially more susceptible to other environmental stresses due to increased levels of nutrient limitation.

1. Introduction

Coccolithophores are a widespread calcifying microalgae group that plays a pivotal role in global carbon cycles via both photosynthesis and calcification [1], accounting for about 10% of total ocean productivity [2]. Their calcium carbonate coccoliths can act as ballast to aid the sinking of organic particles, making them major contributors to the export of carbon from oceanic surface waters to the deep ocean [3]. Previous studies have shown that the photo-physiology and calcification processes of coccolithophores are sensitive to climate change, including altered CO_2, pH, light levels, temperature, and nutrient availability ([4–6]). For instance, ocean acidification can facilitate photosynthesis because of an increase in CO_2 availability. However, since high CO_2 concentration is accompanied by elevated hydrogen ion concentrations (decreased pH), their calcification is hampered [7].

The decreased ozone layer of the Earth's stratosphere has led to an increase in solar UV-B exposures (280–315 nm) in the euphotic layer. Furthermore, progressive climate changes can diminish or augment these increased UV-B exposures in different locations [8]. Changes in PAR and UVR exposure significantly influence phytoplankton growth and photosynthesis, which in turn affect primary production in marine ecosystems [9]. The negative effects of high PAR and UVR stress on photosynthetic organisms have been extensively reported (see the review by Bernhard et al. [10] and literature cited therein). For instance, high light stress could cause photoinhibition in microalgae by affecting PSII repair [11,61]. UVR (particularly UV-B) disrupts DNA synthesis [29,36] and PSII reaction centers in phytoplankton, leading to a decrease in growth and photosynthesis [35,37,54]. In addition, UVR can also induce the formation of reactive oxygen species (ROS) [40], indirectly causing damage to cells. However, contradictory results of increased primary production in natural assemblages in the presence of UVR have also been reported [13,72], due to UV-A (315-400 nm) induced enhancement of photosynthetic carbon fixation under low to moderate levels of solar radiation [28]. Wind-driven mixing can also

* Corresponding author at: State Key Laboratory of Marine Environmental Science & College of Ocean and Earth Sciences, Xiamen University, Xiamen, China.
E-mail address: ksgao@xmu.edu.cn (K. Gao).

https://doi.org/10.1016/j.jphotobiol.2021.112368
Received 16 August 2021; Received in revised form 16 November 2021; Accepted 20 November 2021
Available online 23 November 2021

affect UVR effects on phytoplankton photosynthesis due to changes in UVR-related damage and repair processes [73].

To cope with UVR stress, phytoplankton species have developed effective defensive mechanisms against UVR [9]. UV-absorbing compounds (UVACs) such as mycosporine-like amino acids (MAAs) have been widely documented in diatoms, dinoflagellates, coccolithophores, and natural phytoplankton communities to screen off UVR [38,41,74]. In addition, calcification has been demonstrated to play a defensive role against UVR in some algae [60]. It has been shown that the coccoliths of *Emiliania huxleyi* can block about 26% of UVR [30]. However, such protective mechanisms in calcifying algae can be modulated by temperature [23,65], CO_2 [30,32], and nutrients [14]. When combined with reduced nitrogen availability, further exacerbation of UVR-induced inhibition of photosynthesis and growth has been reported in phytoplankton assemblages or typical species [15].

In the contemporary oceans, nitrogen limitation is prevalent in open oceans and has been suggested to be aggravated due to reduced upward transport of nutrients from deeper waters, which is predicted to intensify with progressive ocean warming [16]. Coccolithophores are the dominant mineralized organisms in oligotrophic environments, and their blooms predominantly occur in well-stratified waters, often in mid- and high-latitudes and following a diatom bloom [39,42,50]. This suggests that they are more likely to experience extensive nitrogen limitation along with increased exposures of PAR and UVR within the shoaled upper mixing layer. Lowered availability of nitrate, on the one hand, significantly decreased the growth and photosynthetic rate of coccolithophores [53], and acts synergistically with other stressors [26]. On the other hand, the higher PIC quotas under nitrogen limitation [6] were suggested to be beneficial to avoidance of viral infection and/or high light and UVR stress [52,56]. Nevertheless, it is not well-understood whether coccolithophores increase coccolith thickness to alleviate UVR damage under nitrogen limitation or suffer an aggravated negative effect of UVR like diatoms and dinoflagellates ([43,44]). Coccolithophores grown under nitrogen-sufficient conditions showed decreased photosynthetic and calcification rates with short-term UVR exposure [30]. Nevertheless, higher particulate inorganic carbon quotas and increased levels of UVACs after acclimation to full spectrum of solar radiation were shown to play photoprotective roles against UVR [33]. Consequently, there is a need to look into coccolithophorid response to the combined effects of UVR and nutrients limitation.

In this work, we aimed to examine the combined effects of nitrate limitation and UVR, by growing the ecologically dominant species *G. oceanica* across a range of nitrate levels with or without UVR. We hypothesized that 1) consecutive daily short-term +UVR (PAR + UV-A + B) exposure is harmful to *G. oceanica*, 2) nitrogen limitation may exacerbate the impact of UVR on *G. oceanica*, and 3) UVR can stimulate calcification, protecting the cells against damage.

2. Materials and Methods

2.1. Culture Conditions and Experimental Design

The cultures of the calcifying coccolithophore *G. oceanica* (NIES-1318) were obtained from the National Institute for Environmental Studies in Japan. Experiments were conducted using 300 mL quartz tubes at 20 °C with PAR of approximately 260 μmol photons m^{-2} s^{-1}, under a 12 h / 12 h light / dark cycle. Cultures were grown in sterilized Aquil artificial seawater medium [68] with standard Aquil nutrient concentrations except for nitrate, and were pre-equilibrated at ambient atmospheric CO_2 concentration (400 μatm). Six nitrate concentrations were prepared as 100, 24, 12, 6, and 3 μM. After 3 d pre-culturing at the different nitrate concentrations, cells were semi-continuously grown using fresh seawater medium with an initial cell density of approximately 4000 cells mL^{-1} for at least 12 generations. There were four replicates for 100, 24, 12 and 6 μM nitrate treatments, and five replicates for 3 μM nitrate treatments. Dilutions were carried out every 2 days to ensure cell concentrations did not exceed 6×10^4 cells mL^{-1}, so that carbonate chemistry was stable during the growth period.

At midday during the daily photoperiod, cells were exposed to a solar simulator (Sol 1200 W, Dr. Hönle, Martinsried, Germany) for ~80 min. The quartz tubes were covered with two different types of radiative wavelength cut-off foils, either: 1) 395 nm cut-off foil, transmitting irradiances above 395 nm (Ultraphan UV Opak, Digefra), or 2) 295 nm cut-off foil, transmitting irradiances above 295 nm (Ultraphan, Digefra) [30]. This ensured that the cells were exposed to PAR (PAR-only) or PAR + UV-A + UV-B (+UVR), respectively. On average, all cultures were exposed to ~600 μmol photons m^{-2} s^{-1} of PAR during the daily 80 min-exposure time, while +UVR replicates were also grown under simultaneous exposure to 45 Wm^{-2} UV-A (315–395 nm) and 2.1 Wm^{-2} UV-B (295–315 nm). Cells were exposed in this way every day until the last day. Due to the different growth rates, the incubation time for each treatment was different: 8 days for 100 μM, 10 days for 24, 12, and 6 μM, and 12 days for 3 μM, (Fig. S1). At the end of the experiment, all replicates were sampled for the following measurements, except for the 3 μM nitrate treatments which collapsed on the last day.

2.2. Measurements and Analysis

2.2.1. Growth Rate

Cell density was measured using a particle counter (Z2, Beckman Coulter Inc., Fullerton, CA, USA) before and after dilution. The specific growth rate (μ) was calculated based on the formula $\mu = (\ln N_1 - \ln N_0) / (t_1 - t_0)$, where N_1 and N_0 were the cell concentrations at t_1 and t_0, respectively. The $(t_1 - t_0)$ is 2 days in this case.

2.2.2. Chlorophyll a, Carotenoids and UVACs Content

On the last day of the incubations, the cells (except the 3 μM treatments, which died eventually) were filtered onto GF/F filters (25 mm, Whatman) for determination of chlorophyll *a* (Chl *a*), carotenoids (Car), and UVACs. After filtering, cells were extracted overnight in pure methanol at 4 °C. Before measurement, samples were centrifuged at 6000*g* for 10 min, and then the absorbance of the supernatant was measured from 200 to 800 nm with a scanning spectrophotometer (DU 800, Beckman, USA). The concentrations of Chl *a* and Car were calculated by the equations: [Chl *a*] (μg mL^{-1}) = $16.29 \times (A_{665} - A_{750}) - 8.54 \times (A_{652} - A_{750})$ [59], and [Car] (μg mL^{-1}) = $7.6 \times (A_{480} - A_{750}) - 1.49 \times (A_{510} - A_{750})$ [67], respectively. The UVR induced changes in Car to Chl *a* ratio were calculated as $(\text{Car: Chl } a)_{+UVR} / (\text{Car: Chl } a)_{PAR}$. The main absorption values of UVACs are in the wavelength range of 310–340 nm [71]. In this study, the absorption peak at 328 nm was regarded as the absorptivity of the UVACs in *G. oceanica* after normalization to the Chl *a* absorption. The calculation of UVACs were obtained by the absorptance height_{OD} / Chl *a* or POC (all parameters were normalized to per unit volume).

2.2.3. Fluorescence Parameters

Photosynthetic efficiency [the maximal quantum yield of PSII, Fv/Fm], the effective quantum yield of PSII (YII), and rapid light curves (RLCs) were measured using an XE-PAM (Walz, Germany) before and after exposure to the solar simulator at the final day. Samples were acclimated for 15 min in the dark to measure Fv/Fm, and YII was measured at the actinic light close to the culture light level. The inhibition of PSII due to high PAR or +UVR was calculated as Inh_{PAR} (%) = $(YII_{PAR0} - YII_{PAR1}) / YII_{PAR0} \times 100$ and Inh_{UVR} (%) = $(YII_{+UVR0} - YII_{+UVR1}) / Y(II)_{+UVR0} \times 100$, respectively. In addition, extra UVR-induced inhibition compared with PAR-only was calculated by $(YII_{PAR1} - YII_{UVR1}) / YII_{PAR1} \times 100$. The maximum relative electron transport rate ($rETR_{max}$), apparent electron transfer efficiency (α), and light saturation point (I_k) were obtained by fitting to the equation of Ralph et al. [62].

2.2.4. C and N Analysis

For particulate organic carbon, inorganic carbon and nitrogen (POC, PIC, and PON) analyses, GF/F filters were pre-combusted at 450 °C for 5 h. On the final day, duplicate samples were filtered from one tube. The one used for POC analysis was fumed with HCl for 12 h, and the other for total particulate carbon (TPC) analysis was not treated with HCl. All samples were dried at 60 °C for about 12 h, and then measured using the Elementar Vario EL cube (Germany). PIC content was obtained by subtracting POC from TPC content. The production rates (P) of PON, POC, and PIC were calculated by multiplying the corresponding cellular contents by μ (d^{-1}), respectively.

2.3. Data Analysis

2.3.1. Fitting of Dose-Response Curves

The dose-response curves of growth vs. nitrate concentrations for PAR-only and +UVR treatments were fitted to the Michaelis-Menten function [51]. Nitrate concentrations were estimated based on the cellular PON quotas, cell concentrations, and the volumes of renewed culture medium (Table S1). And the specific growth rates corresponded to the nitrate concentrations at t_1. It should be noted that we assumed the removed nitrate ions from the cultures were completely assimilated into cellular PON, though this assumption may be violated under high levels of light [47] and ample nitrate availability [46]. In the present study, considering the moderate light level and the low cell abundance, the release of NO_3^- from cells could be negligibly low.

Two-way analysis of variance (ANOVA) was used to test the differences of nitrate concentrations (five levels), irradiance spectrum (two levels) and their interactions among treatments ($p < 0.05$). One-wany ANOVA was used to test the differences of UVR-induced inhibition between different nitrate concentrations ($p < 0.05$). Additionally, a Tukey Post hoc (Tukey HSD) test was used to identify the differences between nitrate concentrations, or irradiance spectra.

3. Results

3.1. Growth Rate and Dynamics during the Whole Culturing Period

The growth rate of *G. oceanica* significantly decreased after 10 generations of acclimation to the corresponding culture conditions when nitrate concentration was lower than 12 μM. However, there were little additional changes between 12 and 100 μM, irrespective of the spectral quality of irradiance (Fig. 2a). Consequently, we regarded 6 and 3 μM as N-limited treatments. The average specific growth rates in these two nitrate treatments after 10 generations of PAR-only growth were 18% (1.01 ± 0.07 d^{-1}) and 45% (0.68 ± 0.19 d^{-1}) lower than the (fitted) maximum growth rate μ_{max} (1.23 d^{-1}, Fig. 1a), respectively. UVR exposure decreased the growth of all the nitrate treatments (Fig. 2a), and the (fitted) maximum growth rate μ_{max} in the presence of UVR was 1.12 d^{-1}, 9% lower than that of PAR-only treatments (Fig. 1). Moreover, UVR growth inhibition increased from 7% to 68% as the nitrate concentration decreased from 100 to 3 μM (Fig. 2b). There were significant interactive effects between UVR and nitrogen limitation on growth rate (two-way ANOVA, $p = 0.0016$, Table S3). The magnitude of this synergistic inhibition of growth was 36–74% higher than that exerted by nitrate limitation or UVR acting independently.

During the whole culturing period, both PAR-only and +UVR cultures maintained relatively stable growth under the nitrate concentrations of 100, 24, and 12 μM, with higher stability after exposure under the solar simulator (Fig. S1 and Fig. S2). In contrast, cells growing under 6 μM and 3 μM nitrate levels gradually failed to reach the initial cell concentrations before dilution, suggesting an accumulation of negative effects in nitrogen-limited treatments under high PAR and +UVR exposure. Relative to PAR-only cultures, growth dynamics of +UVR cultures at 3 μM became more variable across replicates in the latter period. Furthermore, at 3 μM, cultures exposed to extra UVR (8th) collapsed earlier than those grown under PAR-only (12th) conditions, and 100% were dead on the last day.

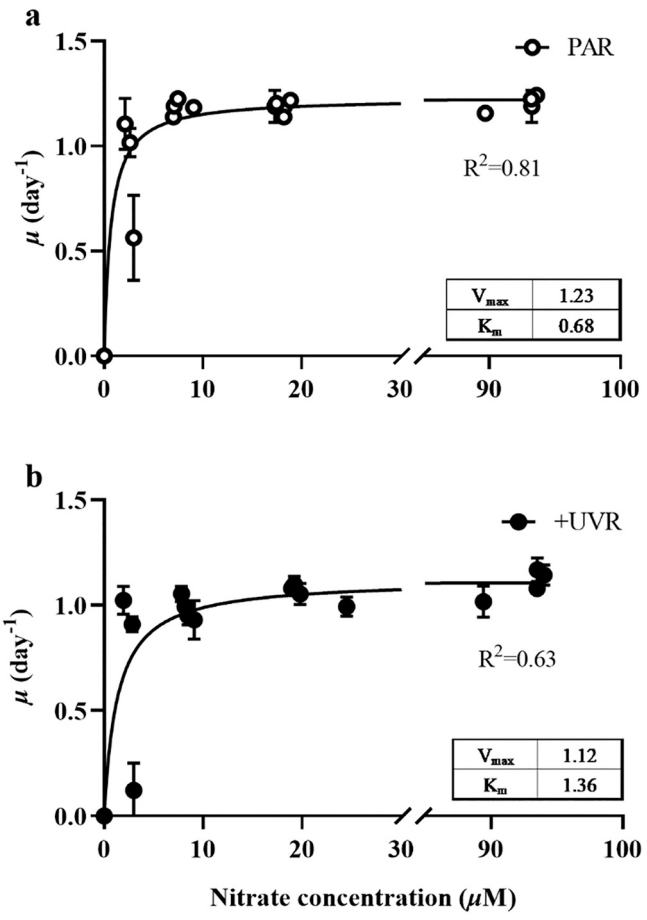

Fig. 1. The relationship between specific growth rates of *G. oceanica* cells and corresponding nitrate concentrations under 80-min (a) elevated PAR and (b) +UVR exposure during the whole culture period. In this figure, values represent the nitrate concentrations before dilutions at every timepoint of the incubations, as calculated in Table S1. The regression line represents the results fitted to the Michaelis-Menten function. Values are the means ± SD of four replicates for 100, 24, 12, and 6 μM, and five replicates for 3 μM.

3.2. Pigments and the Absorptivity of the UV-Absorbing Compounds

In the 6 and 12 μM treatments, the concentration of cellular Chl *a* in both PAR-only and +UVR treatments was significantly lower than at 100 μM (Fig. 3a). There were no significant differences in Chl *a* content between PAR-only and +UVR treatments at all nitrate concentrations ($p > 0.05$). The content of carotenoids showed a similar trend, with lower values at 12 and 6 μM, but higher values in the presence of UVR compared with PAR treatments at 100, 24, and 12 μM ($p > 0.05$, Fig. 3b). The ratio of Car to Chl *a* at 100 and 24 μM in +UVR treatments was higher than that in PAR-only treatments, which was opposite to 6 μM ($p > 0.05$). In addition, the effects of UVR on Car to Chl *a* were highly variable. The UVR induced changes in Car: Chl *a* ranged between 1.12 ± 0.11 and 0.92 ± 0.05, corresponding to a 12% increase or 8% decrease (Fig. 3d), and indicating the higher photo-protection at 100 than 6 μM. The presence of UVR significantly increased UVACs per Chl *a* or per POC at 100 μM and especially in the 24 μM treatments, where the UVACs per Chl *a* or per POC were about two times higher than those in PAR-only treatments. However, this significant increase disappeared in 12 and 6 μM treatments (Fig. 4). In +UVR treatments, the chlorophyll-normalized UVACs contents at 12 and 6 μM were significantly lower

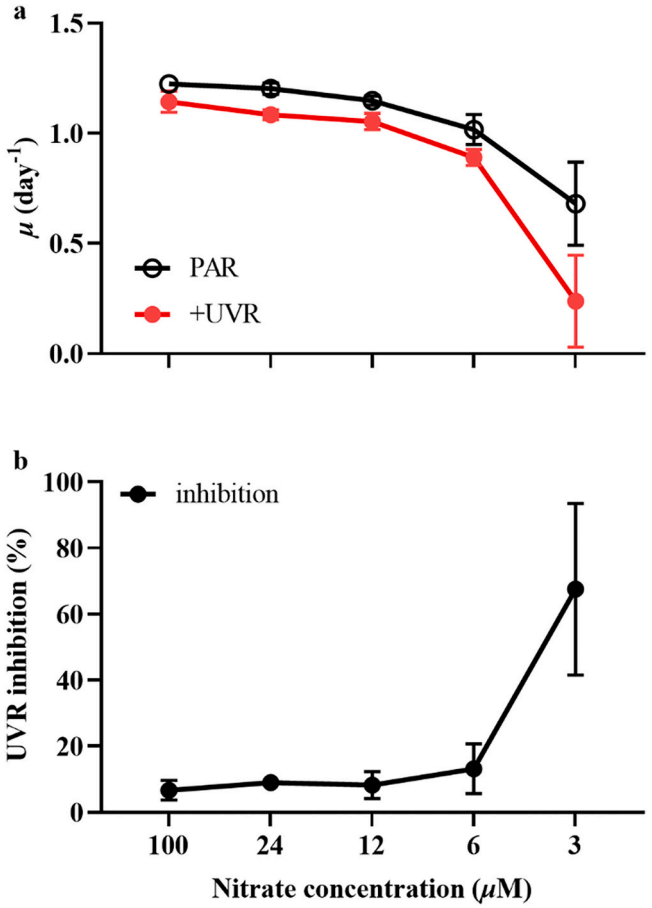

Fig. 2. (a) The average specific growth rates of *G. oceanica* PAR and +UVR cultures after 10 generations, and (b) the UVR inhibition (%) of growth under different nitrate concentrations, calculated as $(\mu_{PAR} - \mu_{+UVR}) / \mu_{PAR} \times 100\%$. Values are the means ± SD of four replicates for 100, 24, 12, and 6 μM, and five replicates for 3 μM.

than that at 100 and 24 μM, and decreased by 38% and 57% when compared with 100 μM. The same trend held for UVACs per POC, which showed a 73% decrease in 6 μM treatments compared with 100 μM treatments. Furthermore, a significant nitrate concentration interaction with irradiance spectrum was observed for both Car: Chl *a* and the concentrations of UVACs (per Chl *a* and per POC) (two-way ANOVA, $p = 0.0007$, $p = 0.0001$ and $p = 0.0015$, Table S3).

3.3. Fluorescence Parameters

The effective quantum yield of PSII (YII) was significantly inhibited at the nitrate concentration of 6 μM on the last day before cells were exposed to the solar simulator. Compared with 24 μM, that YII was reduced by about 24% and 32% in PAR-only and +UVR treatments ($p < 0.0001$, Table S2), respectively. Light spectrum had no significant effect on YII except at 6 μM, which showed a decrease in the presence of UVR ($p < 0.0001$). There were significant interactive effects between UVR and nitrogen concentrations on YII (two-way ANOVA, $p = 0.0019$, Table S3). Furthermore, $rETR_{max}$, I_k, and α were not significantly altered at 24 and 12 μM, but were significantly decreased at 6 μM, and were even lower in the presence of UVR (Table S2).

We also tested the effects of the brief high PAR-only and +UVR exposure on *G. oceanica* directly. After an 80 min-exposure to the solar simulator, YII was significantly decreased in all treatments, with a larger decrease at lower nitrate concentrations and +UVR treatments (Fig. 5b, Table S2), indicating that cells were sensitive to the abrupt increase in

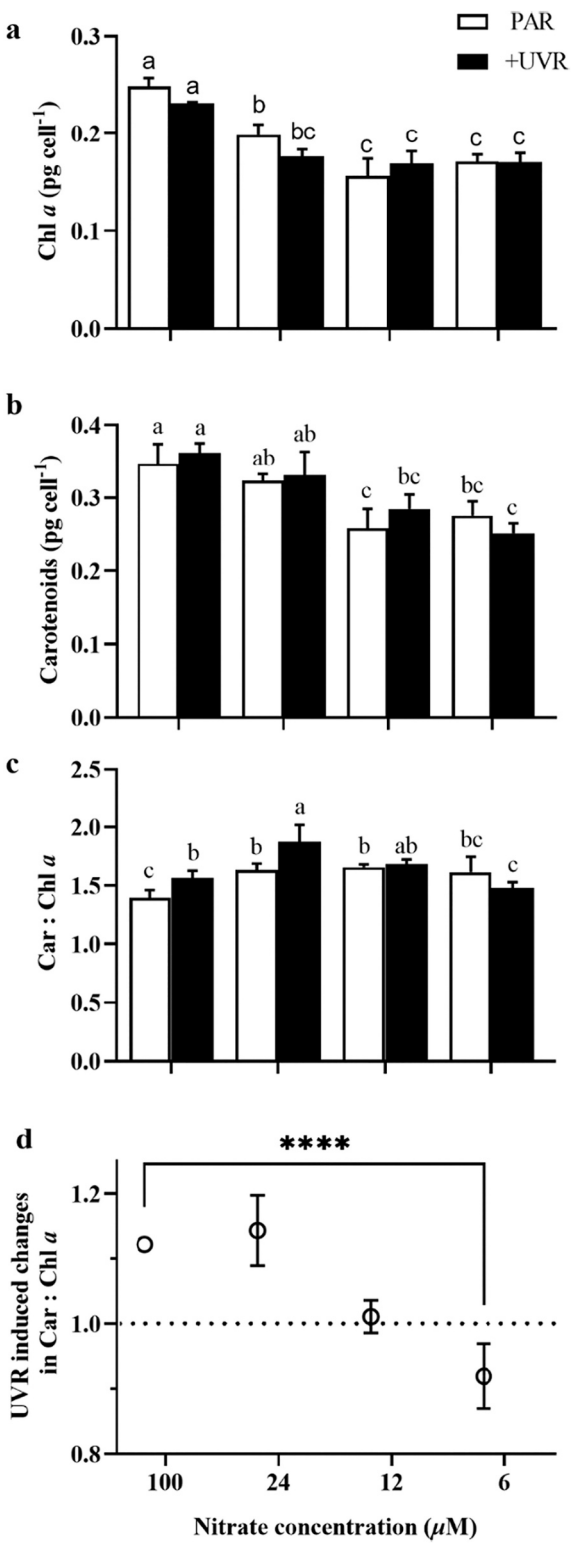

Fig. 3. The cellular contents of (a) Chl *a*, (b) Carotenoids and (c) the ratio of Car: Chl *a* in *G. oceanica* cells grown under different nitrate conditions. (d) The UVR-induced changes in Car: Chl *a* ratios, calculated as $(\text{Car: Chl } a)_{+UVR}$ / $(\text{Car: Chl } a)_{PAR}$. Values are the mean ± SD of four replicates. Different letters indicate significant differences among treatments ($p < 0.05$). **** represents significance levels at $p < 0.0001$.

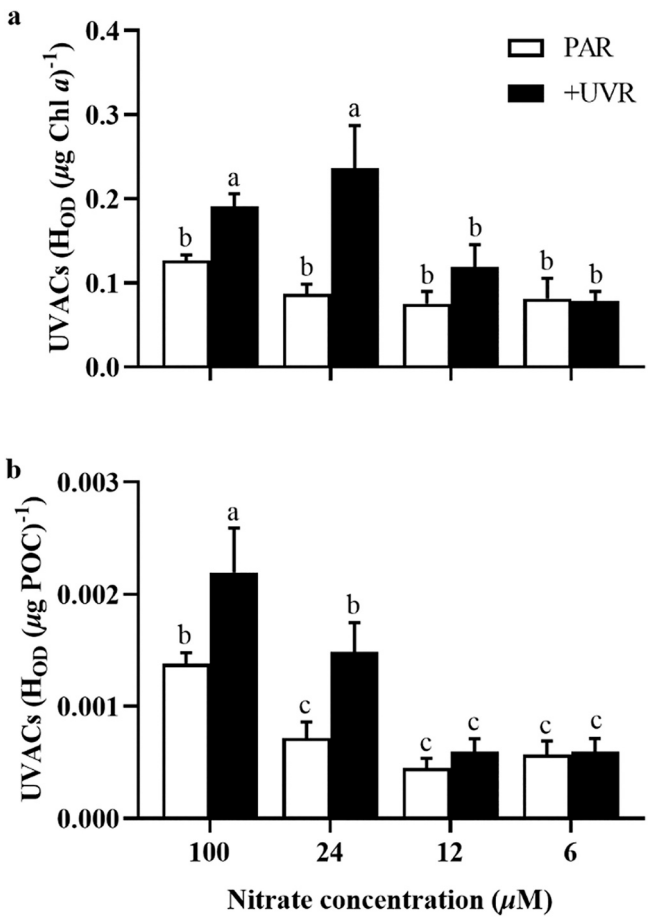

Fig. 4. Contents of UV-absorbing compounds (UVACs) normalized to (a) Chl *a* content and (b) POC content in *G. oceanica* for PAR and +UVR cultures under different nitrate conditions. Values are the mean ± SD of four replicates. Different letters indicate significant differences among treatments ($p < 0.05$).

the irradiances, which was further aggravated by UVR and N-limitation. Specifically, for PAR-only treatments, high light-induced inhibition was 24%, 33%, and 42% at 24, 12, and 6 μM, respectively. In addition, +UVR further increased the inhibition of high PAR-only, with inhibition of 22%, 23%, and 40% at 24, 12, and 6 μM, respectively (Fig. 5c).

3.4. Cellular C, N Quotas, and Production Rates

There were significantly lower cellular PON quotas in 6 μM cultures than at 100 and 24 μM in PAR-only treatments ($p = 0.0298$ and $p = 0.0425$, Fig. 6a). In the presence of UVR, the decreased cellular PON quotas were not significant ($p > 0.05$). The production rate of PON was lower with decreasing nitrate concentration but was only significantly lower in the 6 and 12 μM nitrate conditions, compared to 100 and 24 μM ($p < 0.05$, Fig. 6b). However, for all cultures, no significant differences existed between the two types of spectral quality of irradiance ($p > 0.05$).

The cellular POC quotas of PAR-only cultures were not significantly different among different nitrate concentrations ($p > 0.05$, Fig. 6c). However, POC quotas of +UVR cultures were significantly lower in 6 μM-grown cells than in the other three nitrate concentrations ($p < 0.05$). Though cellular POC quotas were slightly higher in the presence of UVR, there was no significant difference across 100, 24, and 12 μM ($p > 0.05$). However, for cells grown in 6 μM nitrate, cellular POC quotas showed a different trend, as they were lower in the presence of UVR ($p > 0.05$). The POC production rate showed a similar trend to the cellular POC quotas, in that the value was greatly decreased in 6 μM

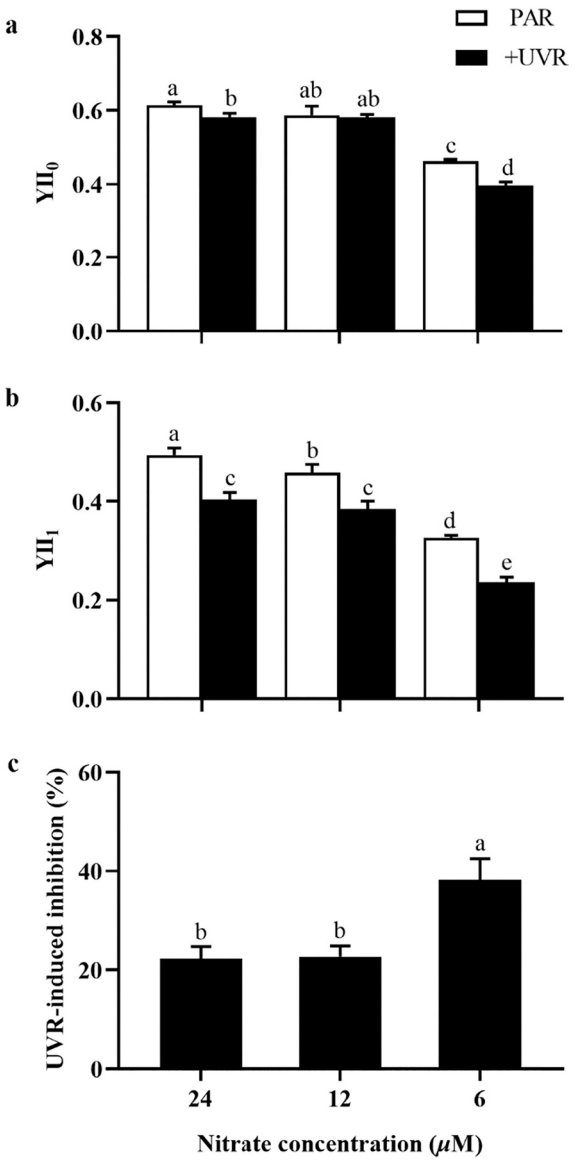

Fig. 5. The effective yield of PSII (YII) of *G. oceanica* (a) before and (b) after high-PAR-only or +UVR exposure (80 min) under different nitrate conditions on the last day of the experiment. (c) The inhibition of +UVR compared with high PAR-only exposure, calculated as ($YII_{PAR1} - YII_{UVR1}$) / $YII_{PAR1} \times 100$. The YII_0 and YII_1 represent yields before or after high-PAR-only or +UVR exposure. Values are the mean ± SD of four replicates. Different letters indicate significant differences among treatments ($p < 0.05$).

nitrate concentration by more than 31% and 45% in PAR-only and +UVR grown cultures, respectively. There were no significant differences in POC production rate between PAR-only and +UVR treatments across the four nitrate treatments of 100, 24, 12, and 6 μM ($p > 0.05$).

The cellular PIC values were not significantly different between PAR-only and +UVR treatments at all the nitrate concentration levels (Fig. 6e). The production rate of PIC at 6 μM was decreased by 43% and 41% in PAR-only and +UVR grown cultures compared with 100 μM, respectively, but not significantly ($p > 0.05$, Fig. 6f) due to the large variability in the replicates.

4. Discussion

Our results confirmed the original hypotheses that UVR would inhibit growth and photosynthetic performance in *G. oceanica*, and that

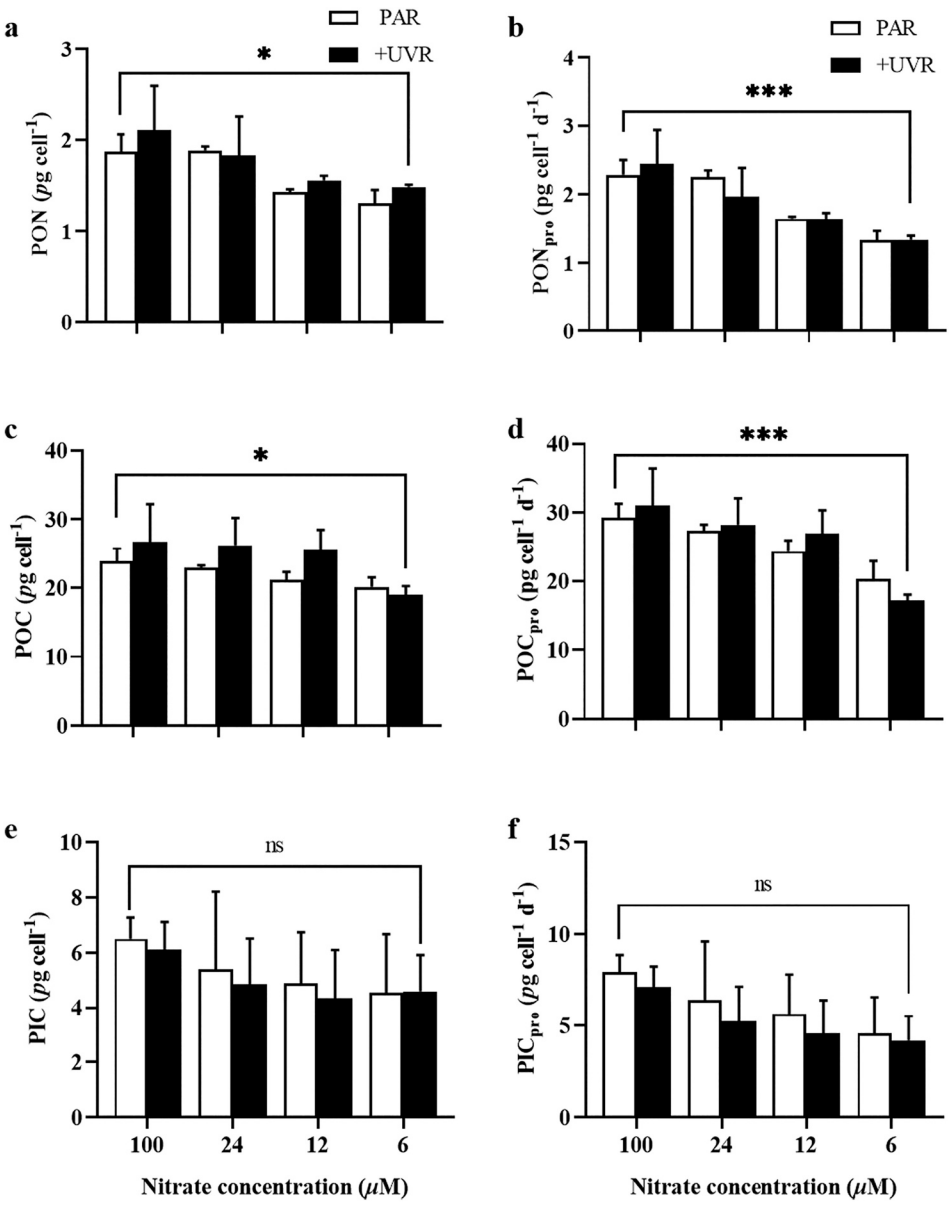

Fig. 6. The cellular (a, b) particulate organic nitrogen (PON) quotas and production rates, (c, d) particulate organic carbon (POC) quotas and production rates, and (e, f) inorganic carbon (PIC) quotas and production rates for PAR-only and +UVR treatments under different nitrate conditions. Values are the mean ± SD of four replicates. *, ***, and ns represent significance levels at $p < 0.05$, 0.001, and > 0.05, respectively.

nitrate limitation would exacerbate these negative effects. The expected increase of PIC in response to UVR was not detected. However, photoprotective pigments, such as carotenoids and UVACs, increased with increased nitrate levels, with such up-regulation presumably being beneficial for *G. oceanica* in resisting UVR-related harm. The strategic trade-offs of energy and resources between calcification and pigment synthesis are thought to play an important role in response to complex environmental fluctuations.

Nitrogen is essential for protein synthesis and thus is extremely important to phytoplankton physiology. Under low nitrate availability, the lack of substrates limits the synthesis of pigments and proteins demanded for photosynthesis and growth. Previous studies have highlighted that limiting nitrogen concentrations decrease photosynthesis by constraining the synthesis of the protein Ribulose-1,5-bisphosphate carboxylase oxygenase (Rubisco) [24], and in this sense, nitrogen limitation directly affects carbon fixation. This is supported by our findings that the growth, yield of PSII, electron transport, Chl *a*, particulate organic carbon, and nitrogen contents decreased at 6 μM compared with 24 and 100 μM nitrate levels. In addition, N-deficiency (6 and 3 μM) induced a much higher inhibition of growth than UVR (Fig. 2a). Recently, it has been reported that the reduced availability of nitrate caused a much greater degree of growth inhibition in *E. huxleyi* than other factors such as ocean acidification [25], which is supported by the present work in terms of comparative effects of UVR and nitrate limitation.

Our results reveal the significance of nitrate availability in the cells' defense against UVR and repairing the UV-related damages. The exposures to UVR hampered the growth of *G. oceanica* (Fig. 2), being consistent with the results on *E. huxleyi* whose growth was inhibited by UVR when grown under natural fluctuations of solar radiation [74]. Such detrimental effects of UVR on growth have also been reported in diatoms and dinoflagellates [48] and phytoplankton assemblages [45]. UVR-induced reduction in growth could be partially due to the damages to the PSII center [18] even under nitrate-replete conditions, though the cells were only exposed to consecutive daily short-term (80 min) UVR exposure (Fig. 5b). Nevertheless, the +UVR treatments maintained

stable growth for the whole period in N-sufficient cultures (Fig. S2). This suggested a strategy of sacrificing growth to defend against UVR-induced harm, exhibiting a damage-repairing balance, which is closely related to nitrogen availability.

Under N-sufficient conditions, the increased levels of UVACs in the presence of UVR indicated induction of photoprotection against UVR in *G. oceanica* (Fig. 4). The higher cellular PON and POC quotas in +UVR treatments also indirectly reflected the higher protection and repair taking place under N-sufficient conditions, because the operation of these processes requires proteins and energy. Furthermore, the higher ratio of Car to Chl *a* in the cells exposed to UVR at 100 and 24 μM (Fig. 3c) suggested another protective mechanism in *G. oceanica*. Carotenoids can dissipate excess light energy through the xanthophyll cycle [22], and exhibit high antioxidant activity to protect the photosynthetic apparatus from damage by ROS [66]. An increased energy dissipation through the xanthophyll cycle was shown in *E. huxleyi* cells when exposed to an abrupt increase in irradiance [63]. In addition, coccoliths are considered to act as a strategic defense against high light and UVR in coccolithophores by dissipating and/or shielding off harmful irradiances [57,63]. In parallel, moderate levels of UVR can simulate PIC production under natural solar radiation with UVR [33]. However, there were no significant differences in PIC quotas and production rates between PAR-only and +UVR treatments even under N-sufficient conditions in this study (Fig. 6). Presumably, the short-term UVR exposure was insufficient to induce significant changes in PIC quotas. Moreover, since calcification is an energetically costly process, trade-offs in energy allocation for calcification and synthesis for UV-protective compounds could be responsible.

While most algae synthesize MAAs to shield off UVR, there is no evidence to date to suggest that coccolithophores accumulate MAAs at levels consistent with photoprotection [20]. Nevertheless, the relatively lower levels of UVACs in coccolithophores appeared to play a role of protection against UVR [74]. In the present work with different levels of nitrate availability, the UV-defensive capability of *G. oceanica* was compromised, mainly due to the depressed synthesis of UVACs. This is known to be related to nitrogen levels [44,58], which is consistent with our results. In addition, cellular PIC quotas and production decreased with the decreased nitrate availability, though the differences were not significant due to the large variations of our data. We noted that more coccoliths fell off from the cells grown at 6 μM than under other higher nitrate concentrations, so the calculated PIC per cell at this nitrogen level did not exactly reflect the abundance of coccoliths on each cell. Therefore, the reduced levels of covering coccoliths might make the cells more vulnerable to UVR. While insufficient N supply led to decreased calcification rates of *E. huxleyi* [25] and *G. oceanica* (this work), N-limitation led to increased PIC quotas and production rates in *E. huxleyi* (PML B92/11) [76]. Such discrepancy could be due to different levels of other factors, such as light and temperature. In the present study, the lower PIC quotas under lower nitrate concentrations could partly be attributed to the lower efficiency of the ion transporters associated with calcification [63,64], involving HCO_3^- transportation, Ca^{2+}/H^+ exchange, and ATPase [49]. Moreover, the short-term UVR exposures might have damaged these ion transporters. From another point of view, nitrogen was preferentially allocated to synthesize proteins involved in the PSII complex to ensure efficient light capture as our results showed that the Chl *a* content did not even decrease in the 6 μM-grown cells (Fig. 3a), though its growth decreased significantly. This reflects that *G. oceanica* increased its energy capture efficiency to cope with UVR stress while sacrificing its growth.

The D1 protein is the primary target in PSII for UVR damage and is necessary for PSII repair [55,69]. Low nitrate availability can inhibit the synthesis of the D1 protein, limiting its turnover and repair and thereby increasing sensitivity to UVR. This was substantiated by our result that short-term responses to UVR caused a dramatic drop in the effective quantum yield of PSII (Fig. 5c), with 6 μM-grown cells exhibiting a significant inhibition, which was not recovered following a resumption of low light illumination. This is quite different from the response of the cells grown under sufficient nitrate concentrations. Furthermore, the synergistic effects of N-limitation and UVR significantly decreased cellular POC quotas and its production, indicating the damage to assimilation processes under the N-limited condition. Thus, for cells cultured at 6 μM, reduced growth could be attributed to a combination of inadequate defense and inability to repair in addition to other suppressed physiological performances due to limitation of nitrogen assimilation.

"Stability" is an attribute of a system that reflects its ability to recover to its original state after suffering disturbances [19]. In our study, nitrate availability determined the stability under UVR interference. Being different from the relatively stable growth under N-sufficient treatments (100, 24, and 12 μM) during the whole experimental period (Fig. S1 and S2), N-limitation (6 and 3 μM) plus UVR compromised the resilience, resulting in more variation across replicates in the latter period, and even causing the system to crash (3 μM), accompanied by a final decreased yield of PSII (Fig. 5a). In addition, compared with previous studies in which *G. oceanica* cells could survive at a low nitrate concentration of 3–5 μM at constant PAR levels within a range of 50–400 μmol photons m^{-2} s^{-1} [70], the eventual collapse of the 3 μM-cultures in our experiments confirmed the negative effects of UVR exposure. This suggests that UVR-induced damage was beyond what repairing mechanisms could cope with under nitrogen restriction.

The effects of UVR are not always negative for phytoplankton. In some in situ investigations, moderate levels of UV-A were shown to enhance photosynthetic carbon fixation of coastal natural phytoplankton assemblages [28,31], and to upregulate CO_2 concentrating mechanisms in the diatom *Skeletonema costatum* [27]. In contrast, UV-B seems to be largely deleterious for phytoplankton cells, damaging the PSII center, DNA synthesis and inducing the production of ROS [17,34]. However, positive effects of UV-B have also been documented in a green alga [12] and a cyanobacterium [21]. In coccolithophores, the promoting effects of UV-A or UV-B on growth and photosynthesis have not yet been documented. Different degrees of damage of UVA and UVB on photosynthesis and calcification have also been reported in other strains of *E. huxleyi* [30,33,75]. The differences in UV-A and UV-B effects are also expected to be related to their doses and nutrients availability during growth. Although we did not distinguish the effects of UV-A and UV-B on growth and photosynthesis, our doses of UV-A and UV-B were higher and their ratios were close to that in natural solar radiation in comparison with those in the literatures, resulting in harmful effects of the summed UV irradiances on *G. oceanica*. Additionally, in the present work, both UV-A and UV-B could have harmed more under N-limited conditions, while relatively low-dose UV-A might play positive roles under replete nitrate conditions. Further studies with more focus on the individual effects of UVA or UVB on coccolithophores grown under different nutrients availabilities are therefore expected.

In summary, this study highlights the key role of nitrogen availability in growth, photosynthesis, and defense against UVR in *G. oceanica*. After the acclimation to consecutive daily short-term high PAR and +UVR, interactions between nitrogen limitation and UVR exacerbated damage to a greater extent than any individual factor. Inhibitory or even lethal effects appeared to be due to an inability to defend and repair when nitrogen supply was highly limiting. Our results indicate that pervasive nitrogen limitation in contemporary and future pelagic oceans will synergistically increase the susceptibility of coccolithophores to UVR. This may make them potentially more susceptible to other environmental stresses, resulting in a reduction in POC and PIC production and ultimately decreasing marine biological carbon export.

Author Statement

Xiaowen Jiang and Kunshan Gao designed the experiment. Xiaowen Jiang carried out the experiment with the assistance of Yong Zhang. Xiaowen Jiang wrote the manuscript with contributions from David A.

Hutchins and Kunshan Gao. All authors reviewed and gave their approval for the final manuscript.

Declaration of Competing Interest

The authors declare that they have no competing financial interests or personal relationships that could have appeared to influence the work reported in this paper.

Acknowledgments

The study was supported by National Natural Science Foundation of China (41720104005, 41890803, 41721005). The authors are grateful to the laboratory engineers Xianglan Zeng and Wenyan Zhao and, to the former Ph.D. student Shanying Tong, for their logistical and technical support. The authors declare that they have no conflict of interest.

Appendix A. Supplementary Data

Supplementary data to this article can be found online at https://doi.org/10.1016/j.jphotobiol.2021.112368.

References

[1] D.A. Hutchins, Oceanography: forecasting the rain ratio, Nature 476 (2011) 41–42, https://doi.org/10.1038/476041a.
[2] A.J. Poulton, T.R. Adey, W.M. Balch, P.M. Holligan, Relating coccolithophore calcification rates to phytoplankton community dynamics: regional differences and implications for carbon export, Deep-Sea Res. II Top. Stud. Oceanogr. 54 (2007) 538–557, https://doi.org/10.1016/j.dsr2.2006.12.003.
[3] P. Ziveri, B. de Bernardi, K.-H. Baumann, H.M. Stoll, P.G. Mortyn, Sinking of coccolith carbonate and potential contribution to organic carbon ballasting in the deep ocean, Deep-Sea Res. II Top. Stud. Oceanogr. 54 (2007) 659–675, https://doi.org/10.1016/j.dsr2.2007.01.006.
[4] Y. Feng, M.E. Warner, Y. Zhang, J. Sun, F. Fu, J.M. Rose, D.A. Hutchins, Interactive effects of increased pCO_2, temperature and irradiance on the marine coccolithophore *Emiliania huxleyi* (Prymnesiophyceae), Eur. J. Phycol. 43 (2008) 87–98, https://doi.org/10.1080/09670260701664674.
[5] Y. Zhang, Z. Li, K.G. Schulz, Y. Hu, A.J. Irwin, Z.V. Finkel, Growth-dependent changes in elemental stoichiometry and macromolecular allocation in the coccolithophore *Emiliania huxleyi* under different environmental conditions, Limnol. Oceanogr. 66 (2021) 2999–3009, https://doi.org/10.1002/lno.11854.
[6] I. Zondervan, The effects of light, macronutrients, trace metals and CO_2 on the production of calcium carbonate and organic carbon in coccolithophores - a review, Deep-Sea Res. II Top. Stud. Oceanogr. 54 (2007) 521–537, https://doi.org/10.1016/j.dsr2.2006.12.004.
[7] U. Riebesell, I. Zondervan, B. Rost, P.D. Tortell, R.E. Zeebe, F.M.M. Morel, Reduced calcification of marine plankton in response to increased atmospheric CO_2, Nature 407 (2000) 364–367, https://doi.org/10.1038/35030078.
[8] R.E. Neale, et al., Environmental effects of stratospheric ozone depletion, UV radiation, and interactions with climate change: UNEP environmental effects assessment panel, update 2020, Photochem. Photobiol. Sci. 20 (2021) 1–67, https://doi.org/10.1007/s43630-020-00001-x.
[9] D.-P. Häder, K. Gao, Interactions of anthropogenic stress factors on marine phytoplankton, Front. Environ. Sci. 3 (2015) 14, https://doi.org/10.3389/fenvs.2015.00014.
[10] G.H. Bernhard, et al., Environmental effects of stratospheric ozone depletion, UV radiation and interactions with climate change: UNEP environmental effects assessment panel, update 2019, Photochem. Photobiol. Sci. 19 (2020) 542–584, https://doi.org/10.1039/d0pp90011g.
[11] J. Jeans, D.A. Campbell, M.O. Hoogenboom, Increased reliance upon photosystem II repair following acclimation to high-light by coral-dinoflagellate symbioses, Photosynth. Res. 118 (2013) 219–229, https://doi.org/10.1007/s11120-013-9918-y.
[12] G. Allorent, et al., UV-B photoreceptor-mediated protection of the photosynthetic machinery in *Chlamydomonas reinhardtii*, Proc. Natl. Acad. Sci. U. S. A. 113 (2016) 14864–14869, https://doi.org/10.1073/pnas.1607695114.
[13] E.S. Barbieri, V.E. Villafañ, E.W. Helbling, Experimental assessment of UV effects on temperate marine phytoplankton when exposed to variable radiation regimes, Limnol. Oceanogr. 47 (2002) 1648–1655, https://doi.org/10.4319/lo.2002.47.6.1648.
[14] J. Beardall, C. Sobrino, S. Stojkovic, Interactions between the impacts of ultraviolet radiation, elevated CO_2, and nutrient limitation on marine primary producers, Photochem. Photobiol. Sci. 8 (2009), https://doi.org/10.1039/b9pp00034h.
[15] J. Beardall, S. Stojkovic, K. Gao, Interactive effects of nutrient supply and other environmental factors on the sensitivity of marine primary producers to ultraviolet radiation: implications for the impacts of global change, Aquat. Biol. 22 (2014) 5–23, https://doi.org/10.3354/ab00582.
[16] M.J. Behrenfeld, et al., Climate-driven trends in contemporary ocean productivity, Nature 444 (2006) 752–755, https://doi.org/10.1038/nature05317.
[17] P. Boelen, M. de Boer, G. Kraay, M.J.W. Veldhuis, A.G.J. Buma, UVBR-induced DNA damage in natural marine picoplankton assemblages in the tropical Atlantic Ocean, Mar. Ecol. Prog. Ser. 193 (2000) 1–9, https://doi.org/10.3354/meps193001.
[18] J.N. Bouchard, M.L. Longhi, S. Roy, D.A. Campbell, G. Ferreyra, Interaction of nitrogen status and UVB sensitivity in a temperate phytoplankton assemblage, J. Exp. Mar. Biol. Ecol. 359 (2008) 67–76, https://doi.org/10.1016/j.jembe.2008.02.022.
[19] S. Botton, M. van Heusden, J.R. Parsons, H. Smidt, N. van Straalen, Resilience of microbial systems towards disturbances, Crit. Rev. Microbiol. 32 (2008) 101–112, https://doi.org/10.1080/10408410600709933.
[20] J.I. Carreto, M.O. Carignan, Mycosporine-like amino acids: relevant secondary metabolites. Chemical and ecological aspects, Mar. Drugs 9 (2011) 387–446, https://doi.org/10.3390/md9030387.
[21] Z. Chen, H.-B. Jiang, K. Gao, B.-S. Qiu, Acclimation to low ultraviolet-B radiation increases photosystem I abundance and cyclic electron transfer with enhanced photosynthesis and growth in the cyanobacterium *Nostoc sphaeroides*, Environ. Microbiol. 22 (2020), https://doi.org/10.1111/1462-2920.14836.
[22] B. Demmig-Adams, W.W. Adams III, The role of xanthophyll cycle carotenoids in the protection of photosynthesis, Trends Plant Sci. 1 (1996) 21–26, https://doi.org/10.1016/S1360-1385(96)80019-7.
[23] S.A. Doyle, J.E. Saros, C.E. Williamson, Interactive effects of temperature and nutrient limitation on the response of alpine phytoplankton growth to ultraviolet radiation, Limnol. Oceanogr. 50 (2005) 1362–1367, https://doi.org/10.4319/lo.2005.50.5.1362.
[24] P.G. Falkowski, A. Sukenik, R. Herzig, Nitrogen limitation in *Isochrysis galbana* (Haptophyceae). II. Relative abundance of chloroplast proteins, J. Phycol. 25 (1989) 471–478, https://doi.org/10.1111/j.1529-8817.1989.tb00252.x.
[25] Y. Feng, M.Y. Roleda, E. Armstrong, P.W. Boyd, C.L. Hurd, Environmental controls on the growth, photosynthetic and calcification rates of a southern hemisphere strain of the coccolithophore *Emiliania huxleyi*, Limnol. Oceanogr. 62 (2017) 519–540, https://doi.org/10.1002/lno.10442.
[26] Y. Feng, M.Y. Roleda, E. Armstrong, T.C. Summerfield, C.L. Hurd, P.W. Boyd, Effects of multiple drivers of ocean global change on the physiology and functional gene expression of the coccolithophore *Emiliania huxleyi*, Glob. Chang. Biol. 26 (2020) 5630–5645, https://doi.org/10.1111/gcb.15259.
[27] G. Gao, W. Liu, X. Zhao, K. Gao, Ultraviolet radiation stimulates activity of CO_2 concentrating mechanisms in a bloom-forming diatom under reduced CO_2 availability, Front. Microbiol. 12 (2021), 651567, https://doi.org/10.3389/fmicb.2021.651567.
[28] K. Gao, Y. Wu, G. Li, H. Wu, V.E. Villafañe, E.W. Helbling, Solar UV radiation drives CO_2 fixation in marine phytoplankton: a double-edged sword, Plant Physiol. 144 (2007) 54–59, https://doi.org/10.1104/pp.107.098491.
[29] K. Gao, P. Li, T. Watanabe, E.W. Helbling, Combined effects of ultraviolet radiation and temperature on morphology, photosynthesis, and DNA of *Arthrospira (Spirulina) Platensis (Cyanophyta)*, J. Phycol. 44 (2008) 777–786, https://doi.org/10.1111/j.1529-8817.2008.00512.x.
[30] K. Gao, Z. Ruan, V.E. Villafañe, J.-P. Gattuso, E.W. Helbling, Ocean acidification exacerbates the effect of UV radiation on the calcifying phytoplankter *Emiliania huxleyi*, Limnol. Oceanogr. 54 (2009) 1855–1862, https://doi.org/10.4319/lo.2009.54.6.1855.
[31] L.S. Garcia-Corral, S. Augusti, A. Regudie-de-Gioux, F. Luculano, P. Carrillo-de-Albornoz, P. Wassmann, C.M. Duarte, Ultraviolet radiation enhances Arctic net plankton community production, Geophys. Res. Lett. 41 (2014) 5960–5967, https://doi.org/10.1002/2014gl060553.
[32] C. García-Gómez, M.T. Mata, F.V. Breusegem, M. Segovia, Low-steady-state metabolism induced by elevated CO_2 increases resilience to UV radiation in the unicellular green-algae *Dunaliella tertiolecta*, Environ. Exp. Bot. 132 (2016) 163–174, https://doi.org/10.1016/j.envexpbot.2016.09.001.
[33] W. Guan, K. Gao, Impacts of UV radiation on photosynthesis and growth of the coccolithophore *Emiliania huxleyi* (Haptophyceae), Environ. Exp. Bot. 67 (2010) 502–508, https://doi.org/10.1016/j.envexpbot.2009.08.003.
[34] D.-P. Häder, E.W. Helbling, C.E. Williamson, R.C. Worrest, Effects of UV radiation on aquatic ecosystems and interactions with climate change, Photochem. Photobiol. Sci. 10 (2011) 242–260, https://doi.org/10.1039/c0pp90036b.
[35] E. Helbling, V. Villafañe, M. Ferrario, O. Holm-Hansen, Impact of natural ultraviolet radiation on rates of photosynthesis and on specific marine phytoplankton species, Mar. Ecol. Prog. Ser. 80 (1992) 89–100, https://doi.org/10.3354/meps080089.
[36] E.W. Helbling, A.G.J. Buma, M.K. de Boer, V.E. Villafañe, In situ impact of solar ultraviolet radiation on photosynthesis and DNA in temperate marine phytoplankton, Mar. Ecol. Prog. Ser. 211 (2001) 43–49, https://doi.org/10.3354/meps211043.
[37] E.W. Helbling, A.G.J. Buma, P. Boelen, H.J. van der Strate, M.V.F. Giordanino, V. E. Villafañe, Increase in Rubisco activity and gene expression due to elevated temperature partially counteracts ultraviolet radiation–induced photoinhibition in the marine diatom *Thalassiosira weissflogii*, Limnol. Oceanogr. 56 (2011) 1330–1342, https://doi.org/10.4319/lo.2011.56.4.1330.
[38] M. Hernando, I. Schloss, S. Roy, G. Ferreyra, Photoacclimation to long-term ultraviolet radiation exposure of natural sub-Antarctic phytoplankton communities: fixed surface incubations versus mixed mesocosms, Photochem. Photobiol. 82 (2006) 923–935, https://doi.org/10.1562/2005-08-29-RA-662.

[39] P.M. Holligan, et al., A biogeochemical study of the coccolithophore, *Emiliania huxleyi*, in the North Atlantic, Glob. Biogeochem. Cycles 7 (1993), https://doi.org/10.1029/93GB01731.
[40] S. Kataria, A. Jajoo, K.N. Guruprasad, Impact of increasing ultraviolet-B (UV-B) radiation on photosynthetic processes, J. Photochem. Photobiol. B 137 (2014) 55–66, https://doi.org/10.1016/j.jphotobiol.2014.02.004.
[41] M. Klisch, R. Sinha, D.-P. Häder, UV-absorbing compounds in algae, Plant Biol. 3 (2002) 113–120.
[42] E.J. Lessard, A. Merico, T. Tyrrell, Nitrate : phosphate ratios and *Emiliania huxleyi* blooms, Limnol. Oceanogr. 50 (2005) 1020–1024, https://doi.org/10.4319/lo.2005.50.3.1020.
[43] M.P. Lesser, J.J. Cullen, P.J. Neale, Carbon uptake in a marine diatom during acute exposure to ultraviolet radiation: relative importance of damage and repair, J. Phycol. 30 (1994) 183–192, https://doi.org/10.1111/j.0022-3646.1994.00183.x.
[44] E. Litchman, P.J. Neale, A.T. Banaszak, Increased sensitivity to ultraviolet radiation in nitrogen-limited dinoflagellates: photoprotection and repair, Limnol. Oceanogr. 47 (2002) 86–94, https://doi.org/10.2307/3069122.
[45] M. Llabrés, S. Agustí, Effects of ultraviolet radiation on growth, cell death and the standing stock of Antarctic phytoplankton, Aquat. Microb. Ecol. 59 (2010) 151–160, https://doi.org/10.3354/ame01392.
[46] M.W. Lomas, P.M. Glibert, Comparisons of nitrate uptake, storage, and reduction in marine diatoms and flagellates, J. Phycol. 36 (2000) 903–913, https://doi.org/10.1046/j.1529-8817.2000.99029.x.
[47] M.W. Lomas, C.J. Rumbley, P.M. Glibert, Ammonium release by nitrogen sufficient diatoms in response to rapid increases in irradiance, J. Plankton Res. 22 (2000) 2351–2366, https://doi.org/10.1093/plankt/22.12.2351.
[48] M.A. Marcoval, V.E. Villafañe, E.W. Helbling, Interactive effects of ultraviolet radiation and nutrient addition on growth and photosynthesis performance of four species of marine phytoplankton, J. Photochem. Photobiol. B Biol. 89 (2007) 78–87, https://doi.org/10.1016/j.jphotobiol.2007.09.004.
[49] L. Mackinder, G. Wheeler, D. Schroeder, P. von Dassow, U. Riebesell, C. Brownlee, Expression of biomineralization-related ion transport genes in *Emiliania huxleyi*, Environ. Microbiol. 13 (2011) 3250–3265, https://doi.org/10.1111/j.1462-2920.2011.02561.x.
[50] P.G. Matson, L. Waashburn, E.A. Fields, C. Gotschalk, T.M. Ladd, D.A. Siegel, Z. S. Welch, M.D. Iglesias-Rodriguez, Formation, development, and propagation of a rare coastal coccolithophore bloom, J. Geophys. Res.: Oceans. 124 (2019) 3298–3316, https://doi.org/10.1029/2019jc015072.
[51] L. Michaelis, M.L. Menten, Die kinetik der invertinwirkung, Biochem. Z. 49 (1913) 333–369.
[52] F.M. Monteiro, et al., Why marine phytoplankton calcify, Sci. Adv. 2 (2016), e1501822, https://doi.org/10.1126/sciadv.1501822.
[53] M.N. Müller, A.N. Antia, J. LaRoche, Influence of cell cycle phase on calcification in the coccolithophore *Emiliania huxleyi*, Limnol. Oceanogr. 53 (2008) 506–512, https://doi.org/10.4319/lo.2008.53.2.0506.
[54] P.J. Neale, J.J. Cullen, R.F. Davis, Inhibition of marine photosynthesis by ultraviolet radiation: variable sensitivity of phytoplankton in the Weddell-scotia confluence during the austral spring, Limnol. Oceanogr. 43 (1998) 433–448, https://doi.org/10.2307/2839092.
[55] Y. Nishiyama, S.I. Allakhverdiev, N. Murata, Protein synthesis is the primary target of reactive oxygen species in the photoinhibition of photosystem II, Physiol. Plant. 142 (2011) 35–46, https://doi.org/10.1111/j.1399-3054.2011.01457.x.
[56] E. Paasche, The effect of temperature, light intensity, and photoperiod on coccolith formation, Limnol. Oceanogr. 13 (1968) 178–181, https://doi.org/10.4319/lo.1968.13.1.0178.
[57] E. Paasche, A review of the coccolithophorid *Emiliania huxleyi* (Prymnesiophyceae), with particular reference to growth, coccolith formation, and calcification-photosynthesis interactions, Phycologia 40 (2001) 503–529, https://doi.org/10.2216/i0031-8884-40-6-503.1.
[58] N.K. Peinado, R.T.A. Díaz, F.L. Figueroa, Ammonium and UV radiation stimulate the accumulation of mycosporine-like amino acids in *Porphyra columbina* (Rhodophyta) from Patagonia, Argentina, J. Phycol. 40 (2004) 248–259, https://doi.org/10.1046/j.1529-8817.2004.03013.x.
[59] R.J. Porra, The chequered history of the development and use of simultaneous equations for the accurate determination of chlorophylls a and b, Photosynth. Res. 73 (2002) 149–156, https://doi.org/10.1023/A:1020470224740.
[60] R. Quintero-Torres, J.L. Aragón, M. Torres, M. Estrada, L. Cros, Strong far-field coherent scattering of ultraviolet radiation by holococcolithophores, Phys. Rev. E Stat. Nonlinear Soft Matter Phys. 74 (2006), https://doi.org/10.1103/PhysRevE.74.032901.
[61] M. Ragni, R.L. Airs, N. Leonardos, R.J. Geider, Photoinhibition of PSII in *Emiliania huxleyi* (Haptophyta) under high light stress: the roles of photoacclimation, photoprotection, and photorepair, J. Phycol. 44 (2008) 670–683, https://doi.org/10.1111/j.1529-8817.2008.00524.x.
[62] P.J. Ralph, C.M.O. Macinnis-Ng, C. Frankart, Fluorescence imaging application: effect of leaf age on seagrass photokinetics, Aquat. Bot. 81 (2005) 69–84, https://doi.org/10.1016/j.aquabot.2004.11.003.
[63] J.B.E. Ramos, K.G. Schulz, S. Febiri, U. Riebesell, Photoacclimation to abrupt changes in light intensity by *Phaeodactylum tricornutum* and *Emiliania huxleyi*: the role of calcification, Mar. Ecol. Prog. Ser. 452 (2012) 11–26, https://doi.org/10.3354/meps09606.
[64] J.A. Raven, K. Crawfurd, Environmental controls on coccolithophore calcification, Mar. Ecol. Prog. Ser. 470 (2012) 137–166, https://doi.org/10.3354/meps09993.
[65] C. Sobrino, P.J. Neale, Short-term and long-term effects of temperature on photosynthesis in the diatom *Thalassiosira pseudonana* under UVR exposure, J. Phycol. 43 (2007) 426–436, https://doi.org/10.1111/j.1529-8817.2007.00344.x.
[66] W. Stahl, H. Sies, Antioxidant activity of carotenoids, Mol. Asp. Med. 24 (2003) 345–351, https://doi.org/10.1016/S0098-2997(03)00030-X.
[67] J.D.H. Strickland, T.R. Parsons, A practical handbook of seawater analysis. Pigment analysis, Bull. Fish. Res. Bd. Canada 167 (1968) 49–80.
[68] W.G. Sunda, N.M. Price, F.M. Morel, Trace metal ion buffers and their use in culture studies, Algal Cult. Tech. 4 (2005) 35–63, https://doi.org/10.1007/s13398-0140173-7.2.
[69] S. Takahashi, N. Murata, Glycerate-3-phosphate, produced by CO_2 fixation in the Calvin cycle, is critical for the synthesis of the D1 protein of photosystem II, Biochim. Biophys. Acta 1757 (2006) 198–205, https://doi.org/10.1016/j.bbabio.2006.02.002.
[70] S. Tong, D.A. Hutchins, F. Fu, K. Gao, Effects of varying growth irradiance and nitrogen sources on calcification and physiological performance of the coccolithophore *Gephyrocapsa oceanica* grown under nitrogen limitation, Limnol. Oceanogr. 61 (2016) 2234–2242, https://doi.org/10.1002/lno.10371.
[71] V.E. Villafañe, E.W. Helbling, O. Holm-Hansen, B.E. Chalker, Acclimatization of Antarctic natural phytoplankton assemblages when exposed to solar ultraviolet radiation, J. Plankton Res. 17 (1995) 2295–2306, https://doi.org/10.1093/plankt/17.12.2295.
[72] V.E. Villafañe, K. Gao, P. Li, G. Li, E.W. Helbling, Vertical mixing within the epilimnion modulates UVR-induced photoinhibition in tropical freshwater phytoplankton from southern China, Freshw. Biol. 52 (2007) 1260–1270, https://doi.org/10.1111/j.1365-2427.2007.01762.x.
[73] Y. Wu, K. Gao, G. Li, E.W. Helbling, Seasonal impacts of solar UV radiation on photosynthesis of phytoplankton assemblages in the coastal waters of the South China Sea, Photochem. Photobiol. 86 (2010) 586–592.
[74] T. Xing, K. Gao, J. Beardall, Response of growth and photosynthesis of *Emiliania huxleyi* to visible and UV irradiances under different light regimes, Photochem. Photobiol. 91 (2015) 343–349, https://doi.org/10.1111/php.12403.
[75] K. Xu, K. Gao, V.E. Villafañe, E.W. Helbling, Photosynthetic responses of *Emiliania huxleyi* to UV radiation and elevated temperature: roles of calcified coccoliths, Biogeosciences 8 (2011) 1441–1452, https://doi.org/10.5194/bg-8-1441-2011.
[76] Y. Zhang, F. Fu, D.A. Hutchins, K. Gao, Combined effects of CO_2 level, light intensity, and nutrient availability on the coccolithophore *Emiliania huxleyi*, Hydrobiologia 842 (2019) 127–141, https://doi.org/10.1007/s10750-019-04031-0.